Efficient Bayesian Exploration for Soft Morphology-Action Co-Optimization

Luca Scimeca[1], Perla Maiolino[1] and Fiumiya Iida[1]

***Abstract*— Morphology been shown to be a fundamental aspect of tactile sensing in soft robotics, one that can aid, and indeed enable, complex discrimination tasks. For a robot to change its sensor morphology as well as control appropriately, the parametric search over morphology and control parameters is usually slow and unsuited for real-world applications. We develop a framework based on Bayesian Exploration, to allow a robot to co-optimize both changes in tactile sensing morphology and robot action control, to aid in complex tactile object discrimination tasks. We test the framework by performing object discrimination on a set of eight objects, varying three different physical properties: geometry, surface texture, and stiffness. We integrate a capacitive tactile sensor into a flat end-effector and create three soft silicon-based filters with varying morphological properties. We incorporate the end-effector onto a robotic arm and perform repetitive, parameterized touch experiments, on each object. We show morphing is indeed necessary to dissociate amongst different object properties with the sensor at hand. Moreover, we show the proposed framework can consistently achieve optimal morphology-action configurations in approximately half the time than systematic search over parameters. This work marks a step towards the creation of robots capable of using morphology and action control to actively aid in discrimination tasks.**

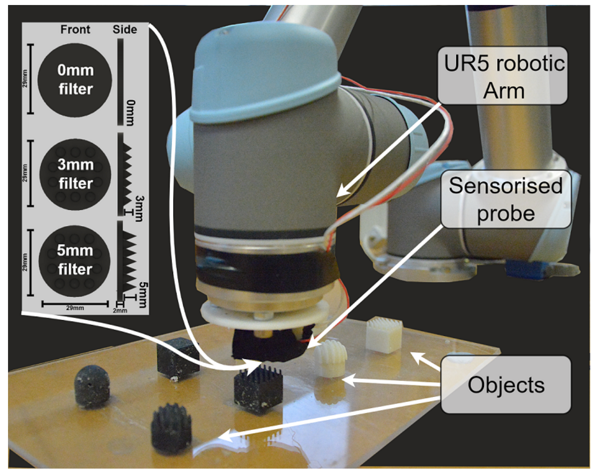

(a) Robot set-up

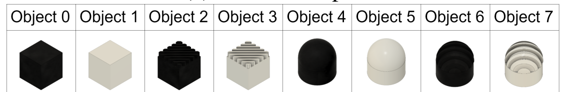

	Object 0	Object 1	Object 2	Object 3	Object 4	Object 5	Object 6	Object 7
Edged	✓	✓	✓	✓	✗	✗	✗	✗
Smooth	✓	✓	✗	✗	✓	✓	✗	✗
Stiff	✗	✓	✗	✓	✗	✓	✗	✓

(b) Designed objects and object properties.

Fig. 1: Experimental set-up for Morphology-Action Co-Optimization.

I. INTRODUCTION

The morphology of the sensory apparatus plays a fundamental role in changing the sensory perception of stimuli arising from interactions with the environment [1]–[3]. In tactile perception this has been observed on a range of biological organisms. For example, the vibrissal system in rats has been shown to be useful in extracting surface features like texture, orientation, size, and more besides. Similarly, the 'Meissner Corpuscles' and 'Dermal Papillae' in humans has been shown to be useful in encoding edge information [4], effectively pre-processing information from the environment into useful stimuli to be further processed by the brain [5]. With the advent of the new generation of (soft) robots [6], [7], the rigidity constraints of the previous century have been loosened, and the possibility of endowing robots with morphing ability has become a reality. Analogously to biological organisms, the sensor morphology in robots can affect the characteristics of the sensed stimuli, and consequently the way in which robots 'perceive' the world [8], [9]. In this context, the intelligent use of (changing) morphology can be fundamental in aiding sensory perception tasks, like object discrimination [10], [11].

Despite these efforts, the role of sensor morphology in encoding and categorizing touch stimuli remains a significant challenge. The interpretation of the sensor signals to discriminate between a set of stimuli or to perform object recognition has relied mainly on supervised machine learning techniques [12]–[14], burdening solutions with the need of expensive computation and large amount of labeled data. In one of our previous studies [11] it was shown how through the use of elastomeric filters as an interface layer between a tactile sensor and the environment, it was possible to perform complex object discrimination with simple clustering analysis, voiding the need for complex learning procedures, and offloading part of the task resolution to the body. The concept of changing morphology has previously been explored [15]–[17], mainly in the context of growth. Here, however, we focus on driving the change in sensor morphology through sensory perception, thus endowing the robot with the ability to autonomously explore its own morphing and motor control abilities and adapt to different categorization tasks.

The main contribution of this paper is to propose a concep-

This work was funded by the UK Agriculture and Horticulture Development Board(Project CP 172)

[1] The authors are with the Bio-Inspired Robotics Lab. Cambridge University Dept. of Engineering, Trumpington St Cambridge CB2 1PZ, UK ls769@cam.ac.uk, fi224@cam.ac.uk

[2] The author is with the Oxford Robotic Institute, University of Oxford, Oxford OX2 6NN, U.K, Email perla@oxfordrobotics.institute

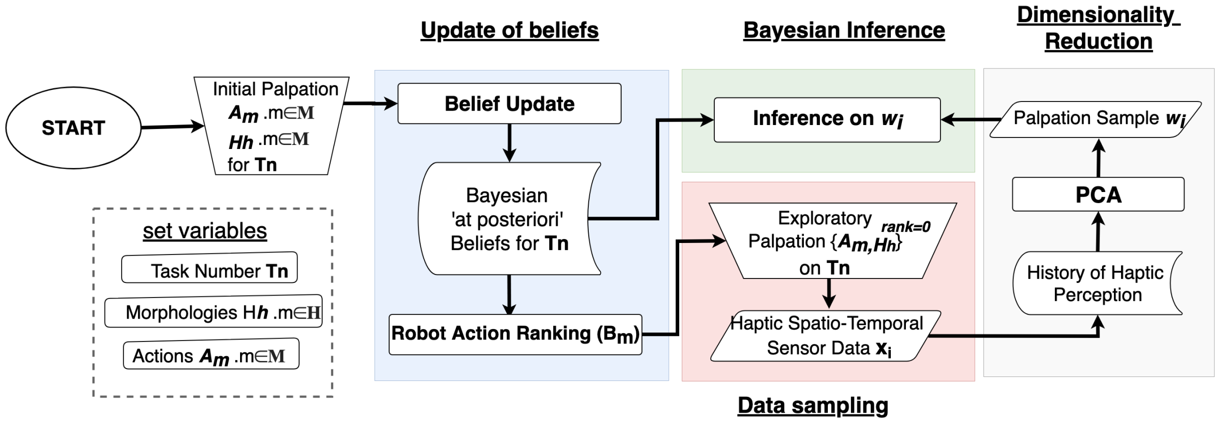

Fig. 2: Flowchart of the developed framework.

tual framework where, through the use of Bayesian Exploration, a robotic agent is capable of exploring the perceptual tactile consequences of both changing sensor morphology and robot control action concurrently. Bayesian Exploration has previously been proposed in [18], and applied for accurate identification of textures and objects in [19]. In this work, additionally to the robot control action, the framework also accounts for the parametric exploration of the robot's soft morphing abilities, to improve detection in complex tactile object discrimination scenarios. To demonstrate this approach, we have developed a set of 8 objects presenting three main surface feature differences, i.e.: geometric (edged vs. non-edged), texture (smooth vs. rough) and elasticity (stiff vs. soft) (Fig. 1).

Firstly, we show how without appropriate morphology, discrimination is often highly non-linear or impossible. Secondly, we show that through the developed framework, the robot is capable of reason probabilistically about the consequence of its own actions, as well as its own morphology, to its sensory perception. The robot is thus capable of meaningfully search its own morphing and action abilities, and avoid the need for expensive systematic search methods. To our knowledge, this is the first application of Bayesian Exploration to enable morphing based on sensor stimuli, and marks a step towards the creation of robots capable of using morphology to actively aid in discrimination tasks.

The paper is organized as follows: In Section II we describe the methods in this paper, including the implemented morphological Bayesian Exploration procedure in Section II-A, the sensor technology in Section II-C and the set-up for the experiments in Section II-B. In Section III the experimental results are presented. Finally, Section IV we provide a discussion and a conclusion.

II. Methods and Experimental Set-up

A. Morphological Bayesian Exploration framework

Bayesian Exploration is an iterative procedure, which can drive the exploration of the robot's morphing and action parametric space within a pre-set task. The proposed framework is comprised of 4 stages: data sampling, dimensionality reduction, Bayesian inference and update of beliefs, and exploratory action identification (Fig. 2). In the last phase, the Bayesian exploratory action identification algorithm implemented is an extension of the one first proposed in [18], to account for morphology exploration during experiments.

1) Data sampling: : Let X be an $(N \times D)$ matrix, where each unique D dimensional row in the matrix is a sequence of tactile images for a touched object, sampled at a constant time interval. The value of N is initially 0 and for each 'experiment iteration' $N = N + K$ where K is the number of classes, or object features to discriminate against.

2) Dimensionality Reduction: After gathering tactile evidence for different objects and obtaining the tactile image sequences matrix X, Principal Component Analysis is used to reduce the dimensionality of the high dimensional spatiotemporal touch evidence. The average tactile sequence for each touch can be computed as:

$$\vec{\mu} = \sum_{i=1}^{n} \vec{x}_i \tag{1}$$

where x_i is a column vector corresponding to the i^{th} row in X. We compute a $(D \times D)$ scatter matrix $\mathbf{S}$ as:

$$\mathbf{S} = \sum_{i=1}^{N} (\vec{x}_i - \vec{\mu})(\vec{x}_i - \vec{\mu})^T \tag{2}$$

Let $\vec{p}_1$ and $\vec{p}_2$ be the eigenvectors of $\mathbf{S}$, corresponding to the two largest eigenvalues. We form a $(D \times 2)$ matrix:

$$\mathbf{\Gamma} = \left[\vec{p}_1{}^T, \vec{p}_2{}^T\right] \tag{3}$$

where $\vec{p}_1{}^T$ and $\vec{p}_2{}^T$ are column vectors in $\mathbf{\Gamma}$. Finally, we project the row vectors in $\mathbf{X}$ onto a 2D subspace by:

$$\mathbf{W} = \mathbf{X} \cdot \mathbf{\Gamma} \tag{4}$$

where $\mathbf{W}$ is a $(N \times 2)$ matrix, and each row w_i is a 2D encoding of a tactile image sequence for an object.

3) Bayesian inference and update of beliefs: As the robot touches an object, the type of surface under touch C, the type of robot control action A and the sensor morphology H generate an observable sensor measurement w_i. The likelihood that a specific surface $C_k \in C$ has generated the haptic observation w_i can thus be computed as:

$$P(C_k|w_i, A_m, H_h) = \frac{P(w_i|C_k, A_m, H_h)P(C_k)}{P(w_i|A_m, H_h)} \tag{5}$$

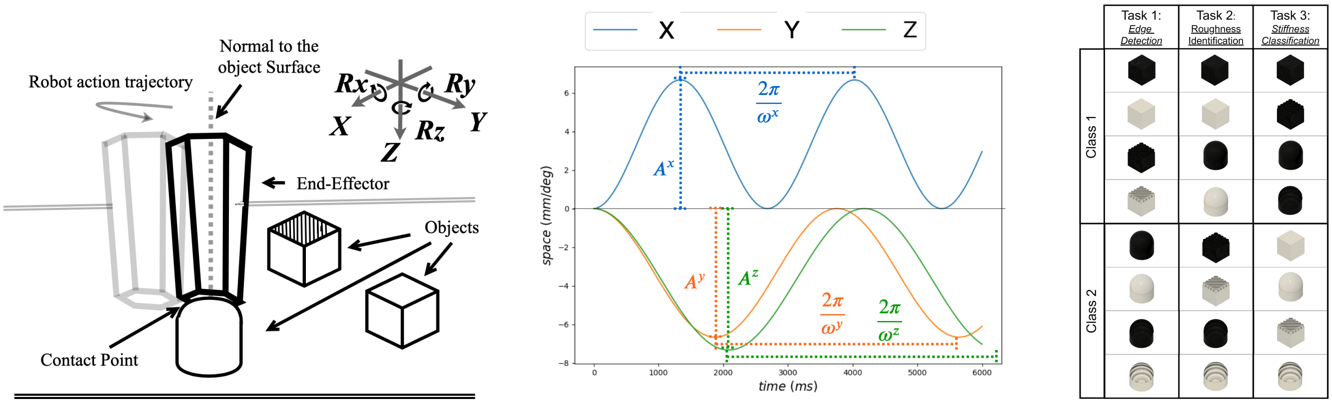

(a) Robot Action Diagram.

(b) Robot Control Profile.

(c) Experimental Tasks.

Fig. 3: Robot control action and experimental tasks.

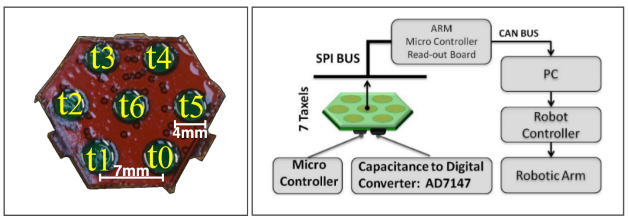

Fig. 4: CySkin capacitive tactile sensor used for the experiments, and sensing architecture.

H_h is a particular morphology and A_m is a specific touch control action. According to the central limit theorem we can approximate the conditional probability of observing w_i, with the probability density function $p(w_i|C_k, A_m, H_h)$, defined by a mean $\vec{\mu}_{k,m,h}$ and a covariance matrix $\mathbf{\Sigma}_{k,m,h}$:

$$P(w_i|C_k, A_m, H_h)P(C_k) \propto p(w_i|C_k, A_m, H_h) = \frac{1}{\sqrt{(2\pi)^2|\mathbf{\Sigma}_{k,m,h}|}} e^{-\frac{1}{2}(\vec{x}-\vec{\mu}_{k,m,h})^T \mathbf{\Sigma}^{-1}_{k,m,h}(\vec{x}-\vec{\mu}_{k,m,h})} \quad (6)$$

We will refer to the set of densities for all morphology-action pairs as the belief state of the robot

As the robot forms a belief state, it is possible to perform Bayesian inference with respect to a specific morphology-action pair by simply evaluating a new, unseen, sample w_j under the Gaussian densities $p(w_i|A_m, H_h)$, for each object under that morphology-action pair. The Gaussian with the highest density at w_j is the most probable class for the unseen sample under consideration.

4) Exploratory action identification: We use Bayesian Exploration to identify the exploratory morphology-action pair necessary to update the beliefs of the robot [18]. The estimate of the morphology and the control action which is most likely to discriminate best amongst different object features is the one which minimizes the discriminatory confusion amongst all possible classes under a specific morphology-action pair. One possible measure of confusion between probability density functions is the amount of overlap between them. We use the Bhattacharyya coefficient to compute a confusion probability matrix $\mathbf{\Psi}_{ks,m,h}$ for each possible exploratory action control A and morphology H. Each element in $\mathbf{\Psi}_{ks,m,h}$ is a mutual confusion between any two classes C_k and C_s, and can be computed as:

$$\mathbf{\Psi}_{ks,m,h} = \int \sqrt{p(w_i|C_k, A_m, H_h)p(w_i|C_s, A_m, H_h)} \quad (7)$$

To make the computation possible within the framework we assume normal probability densities in the belief state, reducing the computation to:

$$\mathbf{\Psi}_{ks,m,h} = \sqrt{\frac{2\vec{\sigma}^2_{k,m,h}\vec{\sigma}^2_{s,m,h}}{\vec{\sigma}^2_{k,m,h} + \vec{\sigma}^2_{s,m,h}}} e^{-\frac{(\vec{\mu}_{k,m,h}-\vec{\mu}_{s,m,h})^2}{4\vec{\sigma}^2_{k,m,h}+4\vec{\sigma}^2_{s,m,h}}} \quad (8)$$

where $\vec{\sigma}_{k,m,h}$ is the diagonal vector of $\mathbf{\Sigma}_{k,m,h}$. The $\mathbf{\Psi}$ probability confusion matrix can be used to find the benefit of making an exploratory action A_m with a sensor morphology H_h. We define two different benefit estimation equations: an unbiased benefit estimation $\widehat{\mathbf{B}}_{m,h}$, and a biased exploratory benefit estimation $\mathbf{B}_{m,h}$. The unbiased benefit estimation for action A_m and morphology H_h can be computed as:

$$\widehat{\mathbf{B}}_{m,h} = \sum_k^K \frac{P(C_k)^2}{\sum_s^K \mathbf{\Psi}_{ks,m,h} P(C_s)} \quad (9)$$

And its value will be higher for control actions with class probability density functions with least overlap. The 'confusion' of using a sensor morphology H_h when making an exploratory action A_m is thus $\widehat{\mathbf{B}}_{m,h}$. Furthermore, we define the biased benefit estimation as:

$$\mathbf{B}_{m,h} = 1 - (1 - \widehat{\mathbf{B}}_{m,h})^{\frac{1}{n_{m,h}}} \quad (10)$$

where $\frac{1}{n_{m,h}}$ is the number of times the robot used morphology H_h and action A_m to touch the objects during experiments. The biased benefits are discounted by the number of times the morphology-action pair has already been performed during action exploration, to discourage excessive exploitation and eventually encourage the exploratory update of belief states under less exploited morphology-actions.

B. Experimental Set-Up

We set up experiments to allow the robot to improve its feature discriminative abilities by co-optimizing morphology and robot control action. The touch experiments were performed using a UR5 robot arm, equipped with a probe

		Parameters	Test Acc. (%) (Avg. Test Acc.)
Task1	**Action Control**	$Ax = 3$, $\omega x = 1$ $Ay = 3$, $\omega y = -0.0025$ $Az = 1$, $\omega z = 0.001$	80 % (31.1 %)
	Morphogy	$5mm$	
Task 2	**Action Control**	$Ax = 3$, $\omega x = 1$ $Ay = 3$, $\omega y = -0.0025$ $Az = 1$, $\omega z = 0.001$	100% (47.2%)
	Morphogy	$3mm$	
Task 3	**Action Control**	$Ax = .05$, $\omega x = 1$ $Ay = 1$, $\omega y = 1$ $Az = 1$, $\omega z = 0.001$	75% (29.81%)
	Morphogy	$3mm$	

TABLE I: The table shows the highest test accuracy achieved through the best performing morphology-action pairs after gathering 10 sample evidence of three object for each task category, and testing on 10 tactile samples for a new object.

sensorised with a capacitive tactile sensor array (Section II-C). Fig. 1 shows the experimental setup developed for both the experiments. To modify the sensor morphology, three different dielectric elastomeric layers were explored, each 3D printed with VeroBlack PolyJet Rubber, and presenting a thin circular layer of $2mm$, as well as conical protrusion, spaced $2mm$ from each other, and with varying height of $0mm$, $3mm$ and $5mm$ (Fig. 1a).

We thus create a set of 8 objects, differing in three sets of features. Fig. 1b shows the objects designed for the experiments. Each object is circumscribed by a $20mm \times 20mm \times 30mm$ cuboid, while we simulate roughness by reproducing $3mm$ protrusion spaced at $2mm$ onto the object's top surface. Following the object design it is possible to classify the objects over three sets of different salient features, i.e.: round vs edged objects, objects with rough vs smooth surfaces, and stiff vs non-stiff. The non-stiff objects (Objects 0, 2, 4, 6 Fig. 1b) were 3D printed with VeroBlack rubber. The stiff objects (Objects 1, 3, 5, 7 Fig. 1b) were 3D printed with rigid PLA material.

Each touch experiment consisted of 2 seconds of contact between the sensorised robot end-effector with a target object. We manually taught the robotic arm the x-y location of each object within its work-space, and set the robot starting position with the end-effector aligned normally to the upper surface of the objects. The end-effector was thus driven downward until a touch event was detected by the capacitive tactile sensor at its extremity, whereby the touch experiment would begin (Fig. 3a). The robot was controlled in Cartesian coordinates at $\approx 60Hz$, acting upon the X, Y and Z tool axis simultaneously. Distinct sinusoidal displacements profiles were generated for every axis, each of which was controlled in amplitude and frequency parameters, thus a total of 6 parameters were used to control the robot for each touch experiment, i.e. Ax, Ay, Az, ωx, ωy and ωz (Fig. 3b).

The Ax, Ay, ωx and ωy parameters were set to allow the robot to rub the surface of the objects on a $10mm$ radius from the center, thus $Ax = 3$, $Ay = 3$, $\omega x \in [-0.0025, 0, 0.0025]$ and $\omega y \in [-0.0025, 0, 0.0025]$. Example object touch experiments are shown in the complementary movie S1.

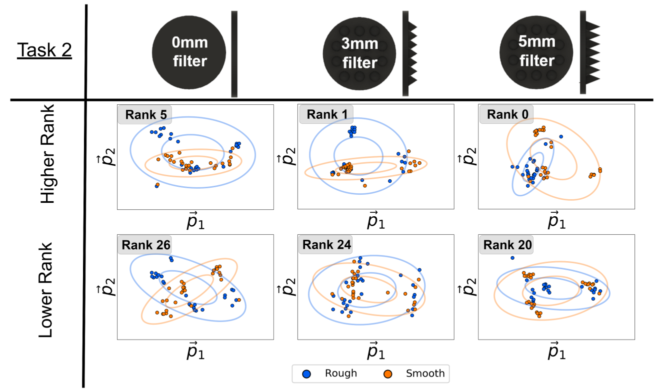

Fig. 5: The robot belief state after 200 iterations for Task 2 (Roughness Identification), under 6 different morphology-action pairs.

C. Sensor Technology

To endow the robot with tactile sensing ability we mount a capacitive tactile sensor, developed in [20], [21] to a custom 3D printed end-effector. The sensor has been integrated into a number of existing robotic systems which exploit sensory-motor co-ordination [22], [23]. The utilized module has a layered structure consisting in a Flexible Printed Circuit Board (FPCB), a dielectric layer and conductive lycra which act as common ground plane for all the taxels and constitute the second plate of the capacitor. the FPCB hosts 7 tactile elements (Taxels), corresponding each to the first plate of a capacitor, and a Capacitance to Digital Converter (CDC AD747 from Analog Devices). The taxels have a diameter of 4mm and a uniform spatial placement with a pitch of $7mm$. The module is connected to a microcontroller board (Intelligent Hub board - IHB) which collects taxels measurement through an SPI bus and processes them before sending them to the PC through CAN-BUS (Fig. 4).

The sensor provides measurement with a resolution of 16 bits corresponding to a variation of capacitance proportional to the surface pressure and is sampled at 50 Hz. A sensor reading, or tactile image, corresponds to a 7-dimensional array, where each element contains the capacitance variation value of the corresponding taxel. To achieve varying sensor morphology we change the dielectric layer of the sensor, thus directly affecting the sensing capabilities of the device.

III. Results

A. Morphology and action for object classification

We assess whether any meaningful filtering can be performed by changing sensor morphology, so to be able to classify each object based on the three tasks: round vs edged objects, objects with rough vs smooth surfaces, and stiff vs non-stiff objects. Systematic touch experiments are performed by varying the robot morphology and action control via every possible action-morphology pair. Each experiment is performed 10 different times, to provide sample evidence for the density distributions in the robot belief state. We can thus test the ability of the robot to classify objects based on the respective task features by forming the density distributions on three of the objects within each feature

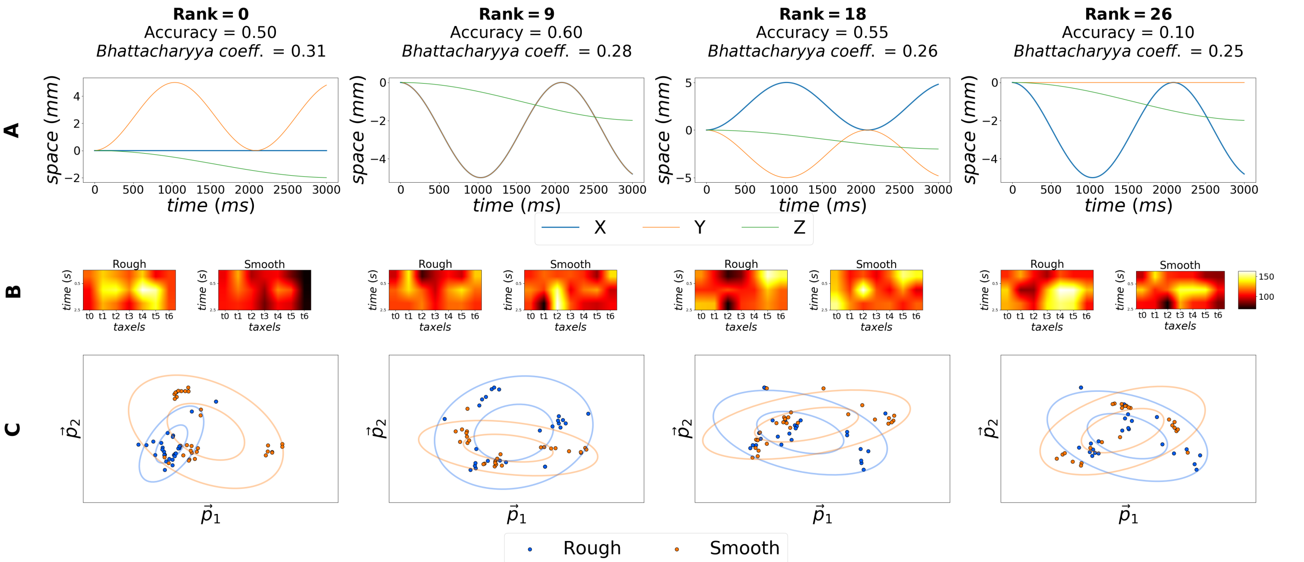

Fig. 6: The ranked morphology-action pairs after approximately 200 iterations on Task 2. Row A shows the action control employed by the robot. Row B shows example raw time series sensor data for each class within Task 2, where the taxels (x-axis) show brighter or darker shades over time (y-axis) depending on the sensed pressure. Finally, row C shows the 2D Gaussians in the belief state of the robot under each action-morphology ranked pair.

set, and performing Bayesian inference (Section II-A) on a random left-out object within it. Table I shows the accuracy achieved for all attempted discriminative tasks. The best morphology-action pairs can achieve accuracy higher than 75% on all tasks. More interestingly, without an appropriate combination of morphology and motor control, it is almost impossible to discriminate objects based on their geometrical, surface roughness or stiffness properties, as shown by the average performance per task by any one pair. Fig. 5 shows the ranked morphology-actions with respect to the unbiased $\widehat{\mathbf{B}}_{m,h}$ benefit estimator for Task 2, roughness identification. The figure shows the relationship between the probability densities formed in the robot belief state, under the developed framework. Highly ranked morphology-action pairs (e.g. Rank 0 and Rank 1) show Gaussian distributions which more easily discriminate between different features, while lower ranked pairs present more distributional overlap, and thus higher degrees of discriminative confusion. Interestingly, although action control can reduce the distributional overlap, the morphology ultimately enables accurate classification (e.g. the distributions of pair Rank 5 vs. pair Rank 0). Varying the morphology, in fact, 'filters' the tactile response [11], inducing sensory differences between objects of varying surface roughness, and enabling discrimination. Fig. 6 shows the ranked morphology-action pairs after approximately 200 iterations on Task 2. The distributional differences between highly and lowly ranked motion are evident within the row sensor data, with morphology-action pairs inducing the sensor data for objects of different classes to be increasingly more distinct (e.g. Rank 0 vs. Rank 26).

B. *Morphological Bayesian Exploration*

We test the Bayesian Exploration framework for morphology-action optimization by running non-systematic experiments and comparing the results to the previous findings. Under the Bayesian exploration framework, the robot is made to touch each object under every morphology-action pair only once, to form an initial belief state. From then on, the robot decides which morphology-action pair to gather additional evidence for, based on the biased estimator ($\mathbf{B}_{m,h}$). Fig. 7 shows the maximal accuracy achieved by the robot during the systematic and Bayesian exploratory experiments. The figure shows how Bayesian exploration consistently outperforms the systematic search over the robot morphology-action parameters, finding good configurations in about half the time necessary to systematic methods.

The fast configuration finding is due to the confusion-driven exploration based on sensor evidence. Assuming distributional consistency amongst sensor values generated under the same conditions, the robot will make informed decisions on which evidence to gather to discriminate the objects with the least amount of confusion at each iteration. The lower accuracy values per task in Table I Section III-A suggest the possibility of overfitting on the objects under touch. Early stopping through cross validational methods can here be used to halt robot training and prevent overfitting.

IV. Discussion and Conclusion

The importance of morphology and sensory-motor coordinated action has been emphasized in the past few decades. In this work, we proposed a Bayesian Exploration framework for a robot to co-optimize the morphology and robot control action to perform object discrimination based on salient features. We show that appropriate control action can aid in object discrimination tasks [11]. More radically, we show that morphology is necessary to enable classification in complex scenario, as it is the case for tactile roughness estimation with our sensor. The appropriate morphing of the dielectric

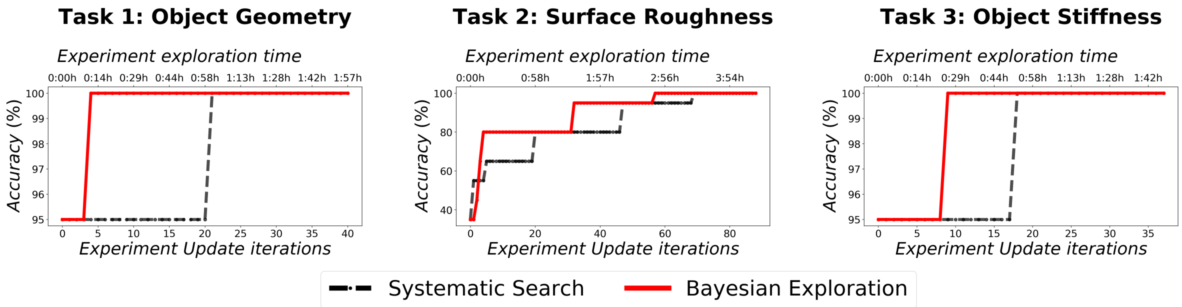

Fig. 7: The figure shows the highest running accuracy for robot throughout the experiments on each task. The developed Bayesian exploration framework consistently out-performs systematic search of morphology-action parameters.

layer, in fact, induces the sensor response to the touching of rough and smooth surfaces to be easily classifiable through Bayesian inference methods. Depending on the employed sensor morphology, instead, almost independently from the control action, the extreme overlap of sensor evidence makes discrimination poor, if not impossible at times.

The Bayesian Exploration framework allows for a reduction in the exploration of parameters, and thus facilitates the real-world parametric exploration of the robot morphing and action capabilities. We show that the robot is capable of finding good morphology-action configurations in approximately half the time necessary to systematic search approach, for each of the attempted tasks.

One limitation of the current approach lies in the parameterization of the robot control action as well as the design of the morphology parameters. As the morphology and control parameters were ultimately human desgined, the fully automation of robot morphing and control is still a far goal. Future work should focus on releasing some of the constraints and biases imposed by human design and aim at automating the generation of solutions, which can be pruned and assessed probabilistically with the proposed framework.

We believe this work can enable the model free, probabilistic, understanding of the consequences of ones actions and body dynamics to the sensory perception derived from interaction with the environment and marks a step towards the creation of robots capable of using morphology to actively aid in tactile discrimination tasks.

REFERENCES

[1] R. Pfeifer, F. Iida, and M. Lungarella, "Cognition from the bottom up: on biological inspiration, body morphology, and soft materials," *Trends in Cognitive Sciences*, vol. 18, no. 8, pp. 404 – 413, 2014.

[2] R. Pfeifer and J. Bongard, *How the Body Shapes the Way We Think*, ser. Computer Science And Intelligent Systems. MIT Press, 2006.

[3] M. Fend, S. Bovet, and R. Pfeifer, "On the influence of morphology of tactile sensors for behavior and control," vol. 54, pp. 686–695, 08 2006.

[4] C. Chorley, C. Melhuish, T. Pipe, and J. Rossiter, "Development of a tactile sensor based on biologically inspired edge encoding," in *2009 Int. Conf. on Advanced Robotics*, June 2009, pp. 1–6.

[5] K. Bagdasarian, M. Szwed, P. M. Knutsen, D. Deutsch, D. Derdikman, M. Pietr, E. Simony, and E. Ahissar, "Pre-neuronal morphological processing of object location by individual whiskers," vol. 16, p. 622, 04 2013.

[6] S. Kim, C. Laschi, and B. Trimmer, "Soft robotics: a bioinspired evolution in robotics," *Trends in biotechnology*, vol. 31, no. 5, pp. 287–294, 2013.

[7] J. Hughes, U. Culha, F. Giardina, F. Guenther, A. Rosendo, and F. Iida, "Soft manipulators and grippers: a review," *Frontiers in Robotics and AI*, vol. 3, p. 69, 2016.

[8] L. Lichtensteiger, "The Need to Adapt and Its Implications for Embodiment," in *Embodied Artificial Intelligence: International Seminar, Dagstuhl Castle, Germany, July 7-11, 2003. Revised Papers*, F. Iida, R. Pfeifer, L. Steels, and Y. Kuniyoshi, Eds. Berlin, Heidelberg: Springer Berlin Heidelberg, 2004, pp. 98–106, dOI: 10.1007/978-3-540-27833-7.

[9] K. Nakajima, H. Hauser, T. Li, and R. Pfeifer, "Information processing via physical soft body," vol. 5, p. 10487, 05 2015.

[10] F. Iida and S. Nurzaman, "Adaptation of sensor morphology: An integrative view of perception from biologically inspired robotics perspective," vol. 6, p. 20160016, 08 2016.

[11] L. Scimeca, P. Maiolino, and F. Iida, "Soft morphological processing of tactile stimuli for autonomous category formation," in *2018 IEEE International Conference on Soft Robotics (RoboSoft)*. IEEE, 2018, pp. 356–361.

[12] P. Gastaldo, L. Pinna, L. Seminara, M. Valle, and R. Zunino, "A tensor-based approach to touch modality classification by using machine learning," *Robotics and Autonomous Systems*, vol. 63, no. Part 3, pp. 268 – 278, 2015, advances in Tactile Sensing and Touch-based Human Robot Interaction.

[13] D. S. Tawil, D. Rye, and M. Velonaki, "Interpretation of the modality of touch on an artificial arm covered with an eit-based sensitive skin," *The International Journal of Robotics Research*, vol. 31, no. 13, pp. 1627–1641, 2012.

[14] M. Kaboli, A. Long, and G. Cheng, "Humanoids learn touch modalities identification via multi-modal robotic skin and robust tactile descriptors," *Advanced Robotics*, vol. 29, no. 21, pp. 1411–1425, 2015.

[15] J. Rieffel, D. Knox, S. Smith, and B. Trimmer, "Growing and evolving soft robots," *Artificial life*, vol. 20, no. 1, pp. 143–162, 2014.

[16] A. Sadeghi, A. Tonazzini, L. Popova, and B. Mazzolai, "A novel growing device inspired by plant root soil penetration behaviors," *PloS one*, vol. 9, no. 2, p. e90139, 2014.

[17] B. Mazzolai, A. Mondini, P. Corradi, C. Laschi, V. Mattoli, E. Sinibaldi, and P. Dario, "A miniaturized mechatronic system inspired by plant roots for soil exploration," *IEEE/ASME Transactions on Mechatronics*, vol. 16, no. 2, pp. 201–212, 2010.

[18] J. A. Fishel and G. E. Loeb, "Bayesian exploration for intelligent identification of textures," *Frontiers in neurorobotics*, vol. 6, p. 4, 2012.

[19] D. Xu, G. E. Loeb, and J. A. Fishel, "Tactile identification of objects using bayesian exploration," in *2013 IEEE International Conference on Robotics and Automation*. IEEE, 2013, pp. 3056–3061.

[20] P. Maiolino, M. Maggiali, G. Cannata, G. Metta, and L. Natale, "A flexible and robust large scale capacitive tactile system for robots," *IEEE Sensors Journal*, vol. 13, no. 10, pp. 3910–3917, 2013.

[21] M. Maggiali, G. Cannata, P. Maiolino, G. Metta, M. Randazzo, and G. Sandini, "Embedded distributed capacitive tactile sensor," 07 2008.

[22] L. Scimeca, J. Hughes, P. Maiolino, and F. Iida, "Model-free soft-structure reconstruction for proprioception using tactile arrays," *IEEE Robotics and Automation Letters*, vol. 4, no. 3, pp. 2479–2484, 2019.

[23] L. Scimeca, P. Maiolino, D. Cardin-Catalan, A. P. del Pobil, A. Morales, and F. Iida, "Non-destructive robotic assessment of mango ripeness via multi-point soft haptics," in *2019 International Conference on Robotics and Automation (ICRA)*. IEEE, 2019, pp. 1821–1826.